

Diode Laser Spectroscopy of Overtone Bands of Acetylene

A. Lucchesini, M. De Rosa, D. Pelliccia, A. Ciucci, C. Gabbanini, S. Gozzini

Istituto di Fisica Atomica e Molecolare del CNR - Via del Giardino, 7 I-56127 Pisa, ITALY

Phone: +39-50/888-126, Fax: +39-50/888-135

E-mail: alex@risc.ifam.pi.cnr.it

Abstract. Overtone absorption lines of acetylene in the regions around 12700 and 11800 cm^{-1} have been examined by the use of tunable diode lasers in free-running mode. The diode laser emission wavelength was scanned around the gas resonances by simply sweeping its injection current, permitting a direct observation of the absorption line-shapes. Weak overtone absorption lines have been detected by using the wavelength modulation (WM) spectroscopy with 2^{nd} harmonic detection technique and the collisional broadening and shift coefficients have been obtained. The high resolving power and accuracy of the spectrometer permitted a wavenumber error of less than 0.01 cm^{-1} . The correct interpretation of the absorption signals when detecting the second harmonic in the presence of a sloping background is discussed.

PACS: 07.65.Gj, 33.70.Jg

The double heterostructure diode lasers (DLs) based on ternary and quaternary compounds emit in the interval between 650 and 1500 nm. In this range the overtone bands of species like CH_4 , C_2H_2 , C_6H_6 , CO , CO_2 , HCl , HCN , HF , H_2O , NH_3 , NO_2 , O_2 , etc. are located. Compared to the lead salt diodes these sources show much simpler operation, mainly because they work at room temperature. On the other hand they cover only the overtone part of the ro-vibrational spectra of the molecules, where the absorption is much weaker than in the fundamental transitions. Overtone and combination of overtone ro-vibrational spectra in the visible and in the near-infrared have been studied more than sixty years ago [1] and recently, by using tunable laser sources, there has been an increasing interest on the spectroscopy of such resonances [2-6]. When a small path-length is a necessity, these weak lines can be still detected by using noise-reduction techniques. For example the frequency modulation (FM) technique [7] can be applied to DLs without any special problem: the modulation of the injection current brings directly to a corresponding emission wavelength variation. When the amplitude of the FM is chosen much lower than the resonance line-width, the FM spectroscopy is usually called wavelength modulation (WM) spectroscopy. Absorptions as weak as from overtone resonances have been successfully observed by using AlGaAs diode lasers [8] by WM spectroscopy and harmonic detection techniques [9].

The gross tuning of these sources is obtained by changing their working temperature from tens of degrees centigrade below zero to tens of degrees above zero. In some cases this permits a tuning through about 10 nm, even if not continuously because of the many DLs mode hops. Unfortunately a change in the injection current causes not only a change in the

emission frequency, but also a variation of the emission power, inducing a typical sloping background where the absorption features have to be extracted from. This inevitably brings to an asymmetry of the collected shapes that must be properly taken into account when fitting the data. In this work the diode laser spectroscopy of some $^{12}\text{C}_2\text{H}_2$ overtone absorption lines is reported, and a critical study of the right analytical approach to the fit of the 2^{nd} harmonic detection of the absorption line-shape is presented. The interpretation of the results when varying the line-width is shown.

1 Experimental Apparatus

Direct absorption and wavelength modulation spectroscopy techniques have been adopted here for pressure broadening and shift measurements. The experimental apparatus for the WM technique is shown in Fig. 1. For this experiment two types of cw diode lasers have been utilized: the SHARP mod. LT024MDO for the $\nu_1 + 3\nu_3$ and $\nu_2 + 3\nu_3 + 2\nu_4$ bands (790 nm), the STC mod. LT50A-03U for the $2\nu_1 + \nu_2 + \nu_3$ band (850 nm). These diode lasers have both single transverse and longitudinal modes. Their current is driven by a stabilized low-noise current generator. The scan of the emission frequency is obtained by adding to the driving current an attenuated low frequency ($\sim 1\text{Hz}$) sawtooth signal coming from an oscilloscope, the same used to display the collected absorption signals. The DL is temperature controlled within 0.002 K by a high-stability temperature controller. The temperature dependence of the diode lasers emission wavelength is linear ($\sim 0.2\text{ nm/K}$), but with mode hops and, for small current variations, the current dependence can be considered linear too ($\sim 0.01\text{ nm/mA}$). The adopted measurement cell is cylindrical, 1 m long and 5 cm in diameter; the laser probe passes up to five times through this cell to

reach a maximum path-length of 5 m. A confocal 5 cm Fabry-Perot interferometer is adopted to mark the frequency scan. A half-meter monochromator is employed for the rough wavelength reading. A sample gas is kept at a fixed pressure in the reference-cell when the system is used for the line-shift measurements. Silicon photodiodes collect the signals, which are then displayed by the oscilloscope. The data acquisition system consists of a desk-top computer equipped with a data acquisition board. It collects, stores and elaborates the measured data.

For the WM spectroscopy a sinusoidal modulation at a frequency of 10 KHz is mixed with the DL injection current. The transmittance is collected by the photodiodes and sent to a single channel lock-in amplifier to extract the first or the second harmonic signal.

2 Line Shape Analysis

The line-shape knowledge is important when studying the pressure-broadening and shift of the absorption features. Therefore let us analyze in detail what are the expected signals when using WM and harmonic detection techniques.

The radiation $I(\nu)$ transmitted through an absorbing gas sample can be described according to the Lambert-Beer equation:

$$I(\nu) = I_o(\nu) \exp[-\alpha(\nu)x] \quad (1)$$

where $I_o(\nu)$ is the incoming radiation intensity at frequency ν , x is the optical density that is the product of the density of the gas by the radiation path-length, $\alpha(\nu)$ is the absorption coefficient. Its shape is heavily influenced by two main phenomena that occur during the absorption process: namely the Doppler-broadening and pressure broadening. The easiest

way to get informations about the absorption line-shape is to apply the DA spectroscopy technique and then to fit the transmitted signal by (1), describing $\alpha(\nu)$ by a function that takes into account the contribution of the Doppler-broadening and the collisional (pressure) broadening altogether. Such a function is the Voigt function, a convolution of the Lorentz and the Gauss curves, given by:

$$f(\nu) = \int_{-\infty}^{+\infty} \frac{\exp[-t^2/(\Gamma_G^2 \ln 2)]}{(t - \nu)^2 + \Gamma_L^2} dt, \quad (2)$$

where ν is the detuning from the gas resonance, Γ_G and Γ_L are the gaussian and lorentzian full-width at half the maximum (FWHM) respectively. In some cases the absorption is so weak that DA spectroscopy does not give enough signal, therefore noise reduction techniques have to be adopted. The WM spectroscopy detects a signal that is not directly the absorption shape, but a function of it. Let us analyze now this functional relation.

The intensity of the detected radiation can be described by:

$$I = F(\nu + k \sin 2\pi\nu' t) \quad (3)$$

where ν' is the modulation frequency and k is the bandwidth. Keeping $k \ll \text{FWHM}$, the (3) can be expanded in Taylor series:

$$I = F(\nu) + kF_1(\sin 2\pi\nu' t) + \frac{k^2 F_2}{2!}(\sin^2 2\pi\nu' t) + \frac{k^3 F_3}{3!}(\sin^3 2\pi\nu' t) + \dots \quad (4)$$

here $F_n(\nu)$ is the n -derivative of $F(\nu)$. By using trigonometrical exemplifications the (4) can be reduced in terms of $\sin(n2\pi\nu' t)$, with $n = 1, 2, 3, \dots$. The multipliers factors for these terms are:

$$n = 1 \implies kF_1(\nu) + \frac{k^3}{8}F_3(\nu) + \frac{2k^5}{960}F_5(\nu) + \dots \quad (5)$$

$$n = 2 \implies \frac{-k^2 F_2(\nu)}{4} - \frac{k^4}{96} F_4(\nu) + \dots \quad (6)$$

$$n = 3 \implies \frac{-k^3 F_3(\nu)}{24} - \frac{3k^5}{2120} F_5(\nu) + \dots \quad (7)$$

They represent the intensity signal when revealing in-phase on the 1st, 2nd and 3rd harmonics respectively. In the followings, the absorption features detected by WM technique have been fitted by functions containing the 1st, 2nd derivative of a good analytical approximation of the Voigt function [10] in order to get the collisional (lorentzian) FWHM and the line center position parameters. The fitting procedure uses a computer program “LINEFIT” set up by D’Amato and one of the authors [11].

The amplitude modulation, which is associated with the emission frequency modulation, results in a sloping background of the direct absorption signal, and in an asymmetry of the 2nd derivative shape in the 2nd harmonic signal. Such an asymmetry involves an apparent displacement of the center of the line, which depends on both the sloping background and the width of the line itself. In particular, the wider is the line, the larger is the apparent displacement, and for instance, in presence of pressure-broadening, an apparent pressure-shift can occur. In order to avoid this “pseudo-shift” and to determine the correct value of the pressure-shift by fitting the experimental data, a proper function that takes into account this emission characteristic of the laser must be used. For this purpose it is useful to better understand how the asymmetry of the signal arises. Let us assume that the sloping signal is the result of multiplying the absorption function $\alpha(\nu)$ by the sloping ramp of the laser power. This is valid only in case of weak absorptions, that is $\alpha(\nu)x \ll 1$, for which the (1) can be approximated by the expansion:

$$I(\nu) \simeq I_o(\nu)[1 - \alpha(\nu)x] \quad (8)$$

Thus, in case of a linear background:

$$I_o(\nu) = \bar{I}_o(1 + s\nu) \quad (9)$$

where \bar{I}_o is the background intensity at $\nu = 0$ and s is the fractional change in the background. Then 2^{nd} derivative of the total signal will be:

$$I''(\nu) = -\bar{I}_o x[(1 + s\nu)\alpha''(\nu) + 2s\alpha'(\nu)] \quad (10)$$

where $\alpha'(\nu)$ and $\alpha''(\nu)$ are the first and the second derivative of the absorption function. It can be verified that the two terms within square brackets have opposite effects on the asymmetry and the second one is predominant. Indeed, when fitting the experimental data, one can be inclined to use simply the 2^{nd} derivative of the absorption function, multiplying it by a sloping linear function in order to match the asymmetry of the experimental signal. The slope of such function has no relation with the physical sloping background, but it is just a mathematical dodge. Although at first sight the quality of the fit could seem satisfactory, i.e. good matching, small residuals, etc., the resulting line parameters (intensity, width and line-center position) could be wrong. In particular the position of the center of the line could be strongly affected by the pseudo-shift. Instead, by using the 2^{nd} derivative of the whole signal (10) as the fitting function, the fit process gives the correct value for the absorption line center, even when the parameters of the linear ramp are not well known. An evidence of the above mentioned misleading results is reported in the next section.

On the contrary, due to the size of the effect, the pressure broadening measurement did not show any strong dependence on which of the fitting function above considered has been taken into account.

3 Experimental Results

Many acetylene absorption lines have been detected by DL spectroscopy. Their wavelengths have been obtained from the measured wavenumbers by using the index of refraction of the air as calculated in the work of Edlén [12]. One example is shown in Fig. 2, where near a well know line a small absorption is present. This could be a rotational line splitting of the R21 by a local perturber via a Coriolis interaction [13]. As already mentioned, it is the amplitude variation of the laser emission that causes the strong asymmetry in the 2^{nd} derivative signal visible in the figure. Two lists of the observed ro-vibrational C_2H_2 absorption lines are reported in Tables 1 and 2, where the band attributions follow the work done by Hedfeld and Lueg [1]. The corresponding vibrational transitions are $\nu_1 + 3\nu_3$ and $2\nu_1 + \nu_2 + \nu_3$ respectively. Considering C_2H_2 a linear symmetric molecule, ro-vibrational transitions between $\Sigma_g^+ \rightarrow \Sigma_u^+$ with $\Delta J = 0$ are not permitted and only transition where $\Delta J = \pm 1$ should occur. Indeed we observed a very weak line at 12675.62 nm, which is shown in Table 1. This is right at the head of the series and can only be attributed to a Q(0). It has been observed in the past by Hedfeld and Lueg [1], even if they classified it as P(0). This can therefore be considered an evidence of a non-perfect linearity of the acetylene molecule.

The $2\nu_1 + \nu_2 + \nu_3$ combination overtone has been previously observed and analyzed by Halonen and co-workers [15] by photoacoustic spectroscopy, and widely analyzed by Temsamani and Herman by using the vibrational *cluster model* [16]. They did not observe any Q branch there. Unfortunately our very sensitive system could not verify it because of the diode laser mode hops. In Table 3 two lines belonging to the $\nu_2 + 3\nu_3 + 2\nu_4$ are reported.

Because of their weakness they have been observed only by the aid of the WM technique. The values of their absorption coefficients at the maximum of the absorption signals are listed in the table in STP conditions. In Fig. 3 three absorption lines are shown as collected by WM and 2nd harmonic technique in the 786 nm range. Two lines are near the 12736.61 cm⁻¹ line listed in Table 3, and even if they certainly are acetylene resonances, their origin and band attribution cannot easily ascribed.

The diode laser spectrometer permits a localization of the resonances with less than 0.01 cm⁻¹. This has been verified many times by multiple measurements of the same spectra and it showed an excellent accuracy. Unfortunately not all the lines belonging to the bands have been found, because of the many mode hops of the diode lasers that have been adopted in these measurements. This characteristic is the major drawback of these sources when used in free-running mode. This problem can be overcome by using external-cavity continuously tunable diode laser systems [17], which we are actually working on.

In our knowledge collisional broadening coefficients for these overtones have not yet been measured, with the exception of the interesting paper of Pavone [6]. Pressure-broadening in air, nitrogen, helium, and the self-broadening coefficients have been measured at room temperature for the isolated and intense 12706.36 (R15) and 12688.71 cm⁻¹ (R5) acetylene lines belonging to the $\nu_1 + 3\nu_3$ band. The results are shown in Table 4. In all the measurements the maximum error in pressure has been estimated to be 5 Torr. For the 12692.67 (R7) and 12703.31 cm⁻¹ (R13) lines the self-broadening coefficients have been obtained too, giving respectively:

$$\gamma_{o(R7)} = (9.4 \pm 0.6) \text{ MHz/Torr}$$

$$\gamma_{o(R13)} = (12.4 \pm 0.6) \text{ MHz/Torr}$$

The result for R7 line is shown in Fig. 4, where an extremely “clean” linear slope can be noted. Self and air-broadening coefficients have also been obtained by Pavone and colleagues [6] in the $\nu_1 + 3\nu_3$ band. In particular for R5 they show similar values within the error. Measurements on the 11765.60 cm^{-1} (P7) line, belonging to the $2\nu_1 + \nu_2 + \nu_3$ band, gave the self-broadening coefficient:

$$\gamma_{o(P7)} = (13.2 \pm 0.6) \text{ MHz/Torr}$$

Self-collisional shift of some acetylene lines has also been measured; the coefficients for R7, R13, 12652.52 cm^{-1} (P9) and 12649.82 cm^{-1} (P10) lines being respectively:

$$S_{R13} = (-0.7 \pm 0.4) \text{ MHz/Torr}$$

$$S_{R7} = (-1.0 \pm 0.1) \text{ MHz/Torr}$$

$$S_{P9} = (-0.6 \pm 0.1) \text{ MHz/Torr}$$

$$S_{P10} = (-0.5 \pm 0.1) \text{ MHz/Torr}$$

In Fig. 5 the result of the measurements for R7 line is shown. A check of the goodness of the fit adopted when using the WM with 2^{nd} harmonic detection technique has been performed on the R21 line shown in Fig. 2. Pressure-shift measurements have been done by using either DA and WM techniques and the results are plotted together in Fig. 6. In this figure the almost perfect parallelism of the best linear fits of the two sets of data shows that they have equal shift coefficients:

$$S_{R21} = (-0.7 \pm 0.2) \text{ MHz/Torr}$$

The drift of the WM data to lower frequency is ought to a systematic phase difference between the two lock-ins used for the differential measurements and it is constant over all the pressure range. The WM data have also been fitted by using the wrong fit function for comparison, in the way described in the previous section. In this case the effect of the pseudo-shift leads to a considerable different value of the shift coefficient, namely -1.1 MHz/Torr .

The 12714.39 cm^{-1} line shown in Fig. 2 is so weak that neither the pressure broadening, nor the shift can be measured by DA. The WM technique comes to help in this situation, but, as said before, the right function along with the best fitting procedure have to be adopted. Therefore for this weak acetylene resonance a sinusoidal 10 KHz modulation has been applied to the DL injection current, and pressure-broadening and shift coefficients have been obtained from the fit of the 2^{nd} harmonic signal coming from the lock-in amplifier:

$$\gamma_o = (12 \pm 1) \text{ MHz/Torr}$$

$$S = (-0.8 \pm 0.5) \text{ MHz/Torr}$$

4 Summary and Conclusions

By using the diode laser spectroscopy it is possible to reveal weak absorptions and also to make specific line-shape measurements under different environmental conditions. Care must be put in correctly analyzing the absorption data, removing the amplitude modulation that comes with the frequency modulation of these sources. The advantage of using DLs as spectroscopic sources lies in the compact dimensions, easy operational characteristics, including the tuning, and the low cost. Compared to the more expensive dye lasers, they show much less noise and better long-time stability. Moreover the resolving power ($\sim 10^7$ in free running mode) permits to discriminate different gases in a complex atmosphere, with response times of a few hundreds of milliseconds. Since DLs can be modulated up to about 10^{10} Hertz, the velocity can be greatly increased with the choice of faster electronics. This can be also a good challenging characteristic for the solid state gas sensors that often need some seconds or even minutes before a quantitative detection result.

WM spectroscopy technique has been used for a sensitivity estimation of the spectrometer constructed in our laboratory. In the wavelength range covered by AlGaAs diode lasers used in this work, the lowest value of the absorption coefficient observable has been $\alpha = 1 \times 10^{-6} \text{ cm}^{-1}$ and the minimum detection limit for C_2H_2 was $2 \times 10^{12} \text{ molecules} \cdot \text{cm}^{-3}$. In favorable conditions, that is at low pressure in a closed cell, and tuning the spectroscopic apparatus on the R15 line of the $\nu_1 + 3\nu_3$ band, some part per million per meter of path-length has been detected; in air at atmospheric pressure 70 ppm per meter of optical length have been revealed. Pressure-broadening and shift measurements have been performed on some of the more intense lines.

Acknowledgments. We are indebted with Prof. G. Alzetta for his precious advice about ro-vibrational transitions. Thanks are due to Mr. M. Badalassi in fabricating the measurement glass cells, and to Mr. M. Tagliaferri for the mechanical construction and set up. One of the authors (De Rosa) wishes to thank the CNR for supporting him with a fellowship.

References

1. K. Hedfeld und P. Lueg: Z. Phys. **77**, 446 (1932)
2. G.J. Scherer, K.K. Lehmann, and W. Klemperer: J. Chem. Phys. **78** , 2817 (1983)
3. Y. Ohsugi, and N. Ohashi: J. Mol. Spectros. **131**, 215 (1988)
4. A. Campargue, M. Chenevier, and F. Stoekel: J. Mol. Spectros. **151**, 275 (1992)
5. J. Sakai and M. Katayama: J. Mol. Spectros. **154**, 277 (1992)
6. F.S. Pavone, F. Marin, M. Inguscio, K. Ernst, and G. Di Lonardo: Appl. Opt. **32**, 259 (1993)
7. G.C. Bjorklund, M.D. Levenson, W. Lenth, C. Ortiz: Appl. Phys. B **32**, 145 (1983)
8. A. Lucchesini, I. Longo, C. Gabbanini, S. Gozzini, and L. Moi: Appl. Opt. **32**, 5211 (1993)
9. J. Reid, and D. Labrie: Appl. Phys. B **26**, 203 (1981)
10. J. Puerta, and P. Martin: Appl. Opt. **20**, 3923 (1981)
11. F. D'Amato and A. Ciucci, ENEA Report **RT/INN/94/01** (1994)
12. K. Eldén: Metrologia **2**, 71 (1966)

13. B.C. Smith and J.S. Winn: J. Chem. Phys. **94**, 4120 (1991)
14. G. Herzberg: *Infrared and Raman Spectra of Polyatomic Molecules*, (Van Nostrand Reinhold, New York 1945), p. 290
15. X. Zhan, O. Vaittinen, and L. Halonen: J. Mol. Spectros. **160**, 172 (1993)
16. M.A. Temsamani and M. Herman: J. Chem. Phys. **102**, 6371 (1995)
17. Q. Nguyen, and R.W. Dibble: Opt. Lett. **19**, 2134 (1994)

Tables

Table 1. List of observed acetylene absorption lines. The transitions are classified according to Hedfeld and Lueg [1], and belong to the $\nu_1+3\nu_3$ overtone band [14]

Wavelength (<i>nm</i>)	Wavenumber (<i>cm</i> ⁻¹)	J number	Branch
786.035	12718.58	24	<i>R</i>
786.124	12717.14	23	<i>R</i>
786.199	12715.93	22	<i>R</i>
786.273	12714.73	21	<i>R</i>
786.355	12713.41	20	<i>R</i>
786.437	12712.08	19	<i>R</i>
786.527	12710.63	18	<i>R</i>
786.615	12709.20	17	<i>R</i>
786.699	12707.85	16	<i>R</i>
786.791	12706.36	15	<i>R</i>
786.861	12705.23	14	<i>R</i>
786.980	12703.31	13	<i>R</i>
787.084	12701.63	12	<i>R</i>
787.190	12699.91	11	<i>R</i>
787.298	12698.18	10	<i>R</i>
787.407	12696.42	9	<i>R</i>
787.516	12694.67	8	<i>R</i>
787.640	12692.67	7	<i>R</i>
787.885	12688.71	5	<i>R</i>
788.010	12686.70	4	<i>R</i>
788.141	12684.59	3	<i>R</i>
788.280	12682.35	2	<i>R</i>
788.407	12680.31	1	<i>R</i>
788.699	12675.62	0	<i>Q</i> ^a
788.842	12673.32	1	<i>P</i>
788.992	12670.93	2	<i>P</i>
789.140	12668.53	3	<i>P</i>
789.326	12665.93	4	<i>P</i>
789.456	12663.46	5	<i>P</i>
790.133	12652.52	9	<i>P</i>
790.308	12649.82	10	<i>P</i>

^a This line is very weak and has been observed also by Hedfeld and Lueg. It corresponds to the head of the series

Table 2. List of observed acetylene absorption lines belonging to the $2\nu_1 + \nu_2 + \nu_3$ overtone band [14]

Wavelength (<i>nm</i>)	Wavenumber (<i>cm</i> ⁻¹)	J number	Branch
848.126	11787.46	1	<i>R</i>
848.836	11777.60	2	<i>P</i>
849.010	11775.19	3	<i>P</i>
849.221	11772.26	4	<i>P</i>
849.555	11767.64	6	<i>P</i>
849.702	11765.60	7	<i>P</i>
849.939	11762.32	8	<i>P</i>
850.115	11759.89	9	<i>P</i>
850.787	11750.60	12	<i>P</i>
850.935	11748.56	13	<i>P</i>
851.219	11744.62	14	<i>P</i>
851.387	11742.31	15	<i>P</i>
852.318	11729.48	19	<i>P</i>
852.651	11724.91	20	<i>P</i>

Table 3. List of observed acetylene absorption lines belonging to the $\nu_2 + 3\nu_3 + 2\nu_4$ overtone band [14]

Wavelength (<i>nm</i>)	Wavenumber (<i>cm</i> ⁻¹)	J number	Branch	α_{max} (<i>cm</i> ⁻¹ / <i>amagat</i>)
784.800	12738.60	10	<i>R</i>	5.6×10^{-6}
784.922	12736.61	9	<i>R</i>	1.9×10^{-5}

Table 4. List of measured acetylene FWHM broadening coefficients for the 12706.36 cm^{-1} (R15) and the 12688.71 cm^{-1} (R5) absorption lines

R5	R15
$\gamma_{\text{o}} = (13.5 \pm 0.1)\text{ MHz/Torr}$	$\gamma_{\text{o}} = (11.0 \pm 0.1)\text{ MHz/Torr}$
$\gamma_{\text{air}} = (8.1 \pm 0.1)\text{ MHz/Torr}$	$\gamma_{\text{air}} = (5.8 \pm 0.1)\text{ MHz/Torr}$
$\gamma_{\text{H}_2} = (8.3 \pm 0.3)\text{ MHz/Torr}$	$\gamma_{\text{H}_2} = (6.6 \pm 0.1)\text{ MHz/Torr}$
—	$\gamma_{\text{He}} = (3.7 \pm 0.2)\text{ MHz/Torr}$

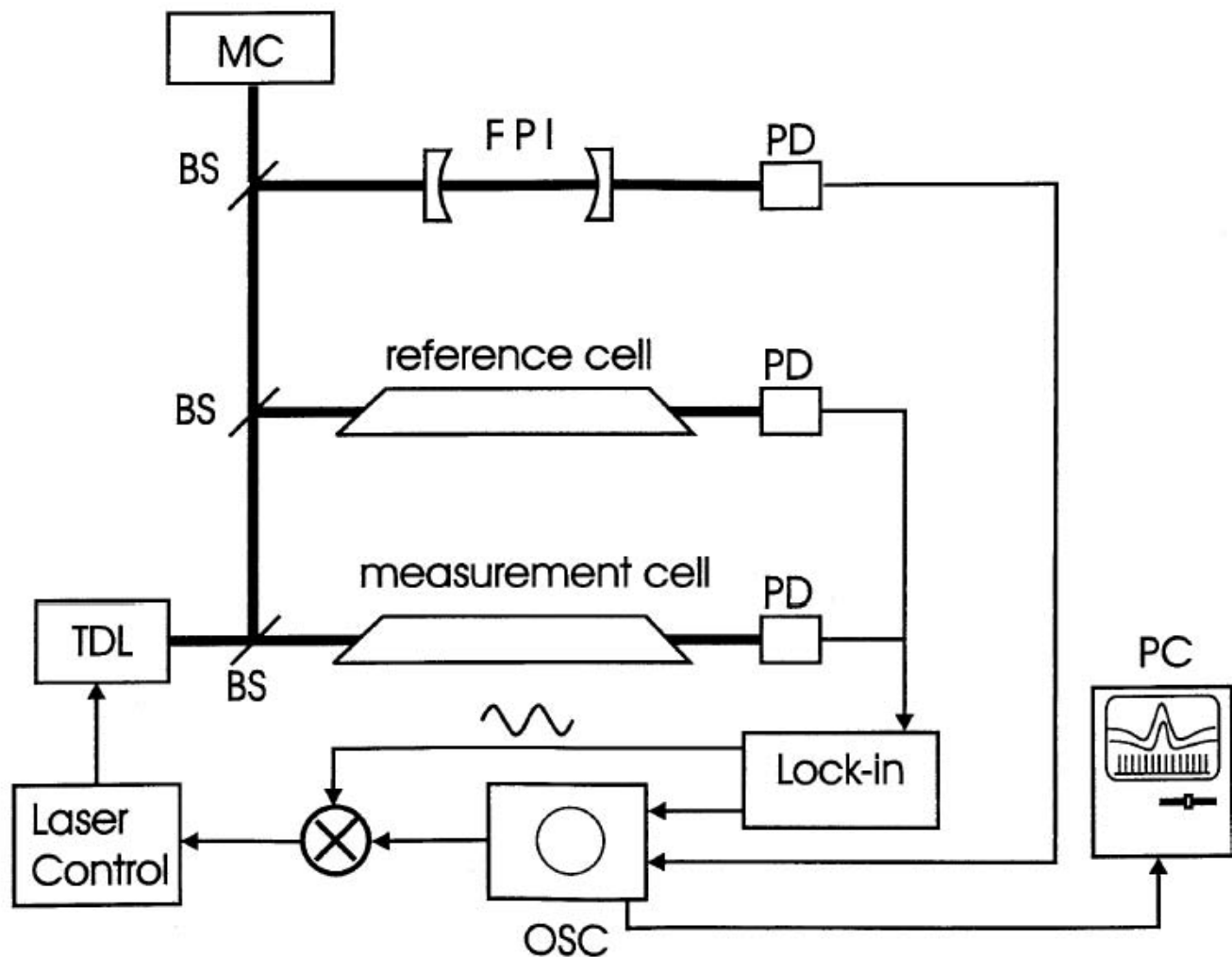


Fig. 1. Sketch of the experimental apparatus for the WM spectroscopy. PD: photodiode; BS: beam splitter; FPI: Fabry-Perot interferometer; TDL: tunable diode laser; MC: monochromator; OSC: oscilloscope; PC: desk-top computer

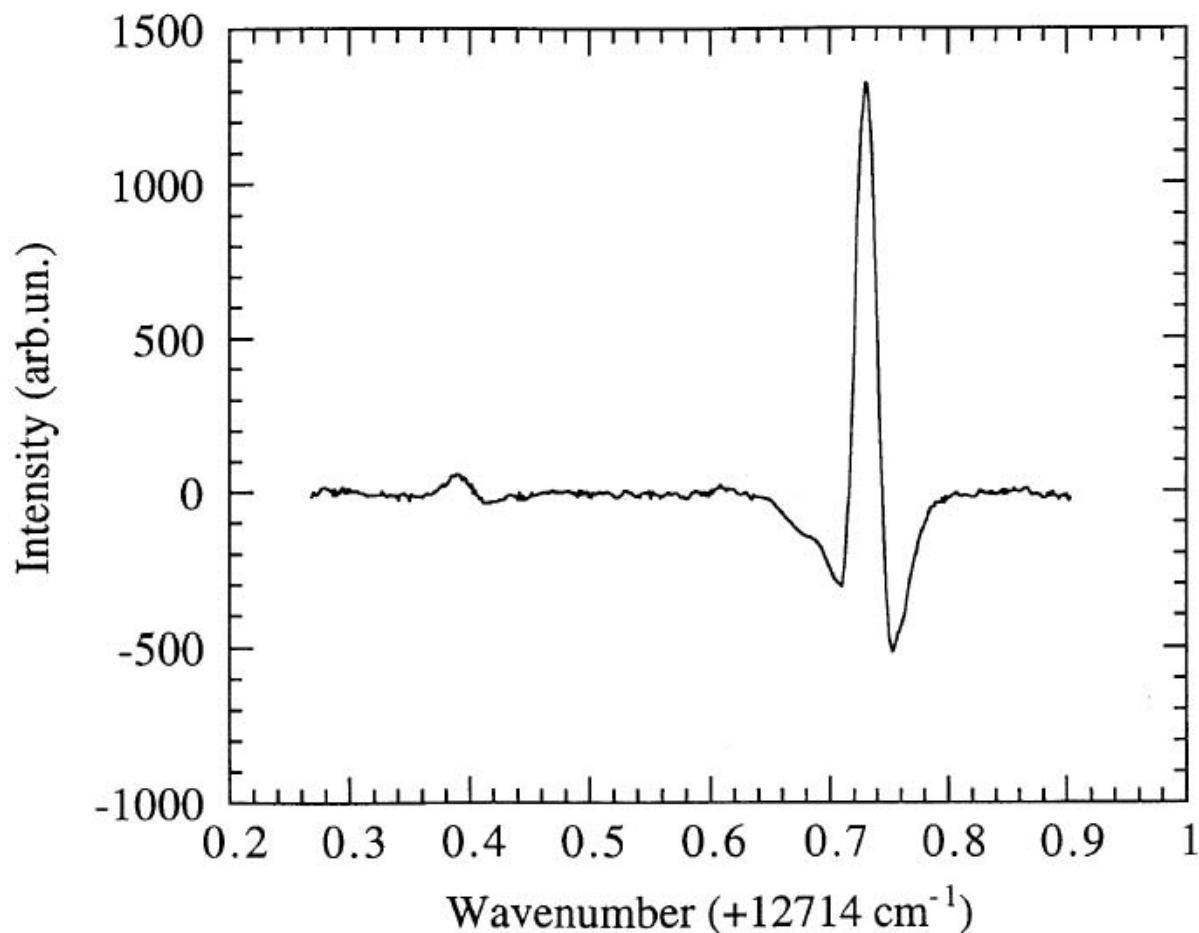


Fig. 2. Two acetylene absorption lines observed by WM spectroscopy and 2nd harmonic detection technique when the gas pressure was 38 Torr. The more intense is located at 12714.73 cm^{-1} ($\nu_1 + 3\nu_3$, R21, 786.273 nm @ 15°C). The other, whose origin is suggested in the text, has its minimum at 12714.39 cm^{-1} (786.294 nm @ 15°C). The lock-in time constant was 12.5 ms

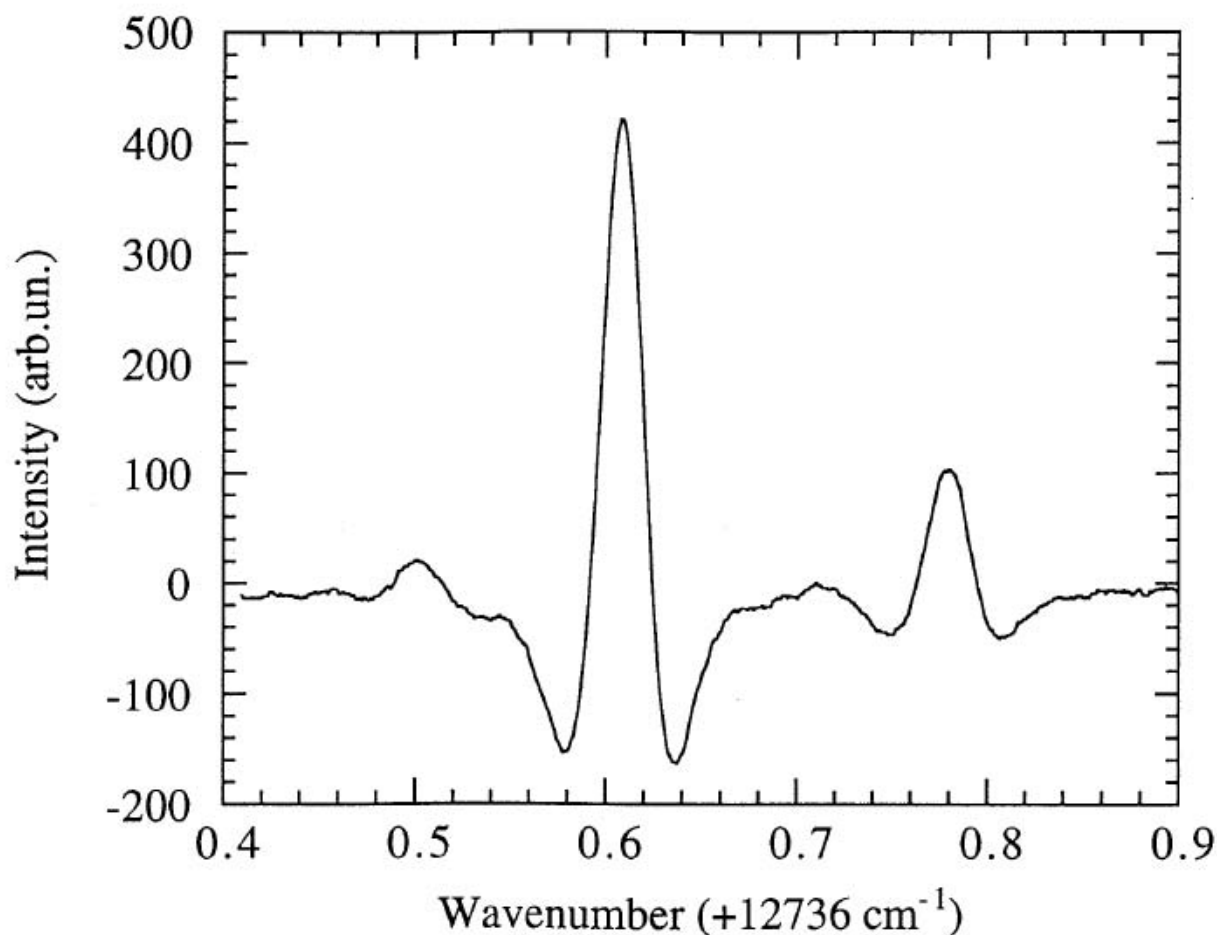


Fig. 3. Three acetylene absorption lines observed by WM spectroscopy and 2nd harmonic detection technique. Near the 12736.61 cm^{-1} line ($\nu_2 + 3\nu_3 + 2\nu_4$, P9, 784.922 nm @ 15°C) two new lines are shown at 12736.50 and 12736.78 cm^{-1} . The gas pressure was 40 Torr and the lock-in time constant was 12.5 ms

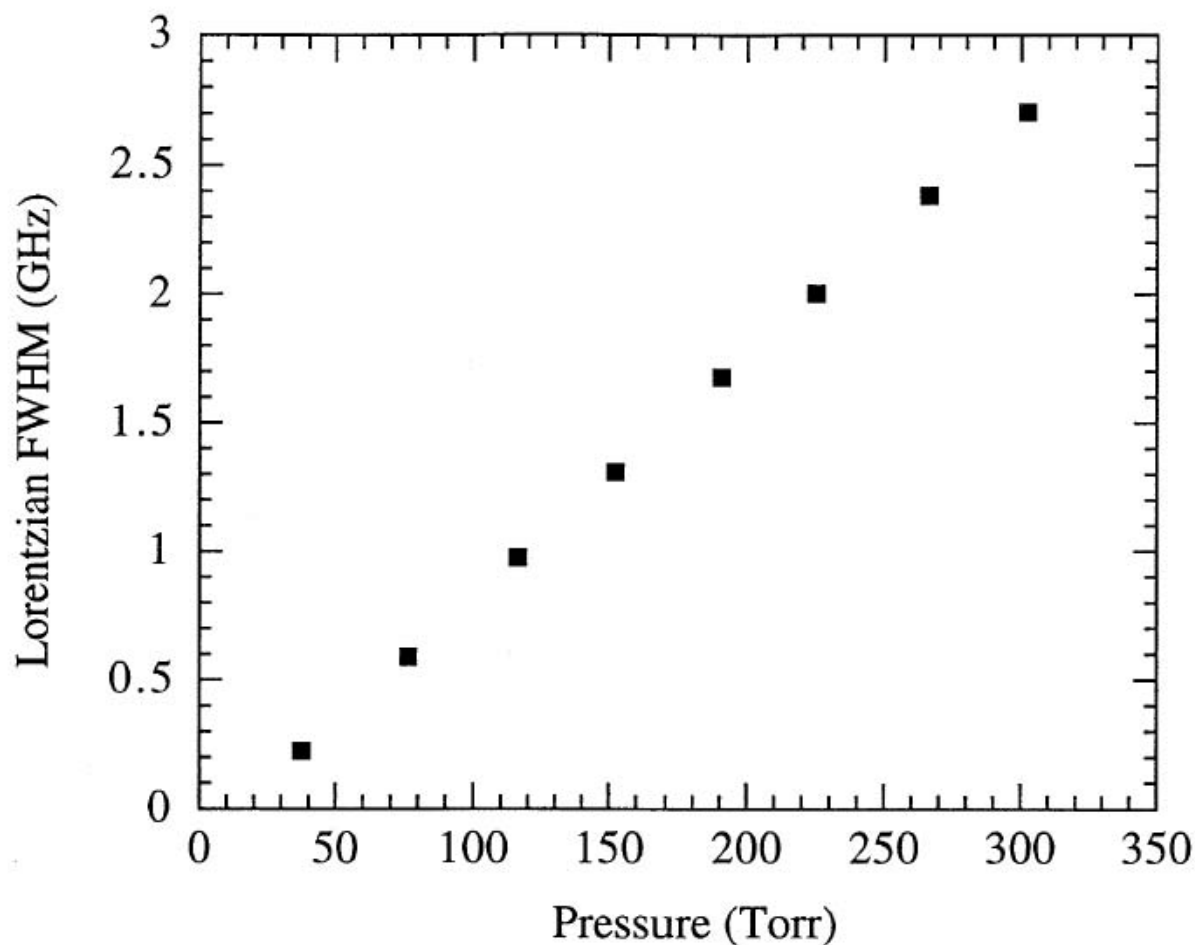


Fig. 4. Self-broadening data related to the 12692.67 cm^{-1} ($\nu_1 + 3\nu_3$, R7, 787.640 nm @ 15°C) C_2H_2 overtone absorption line. The error in pressure measurement was 5 Torr

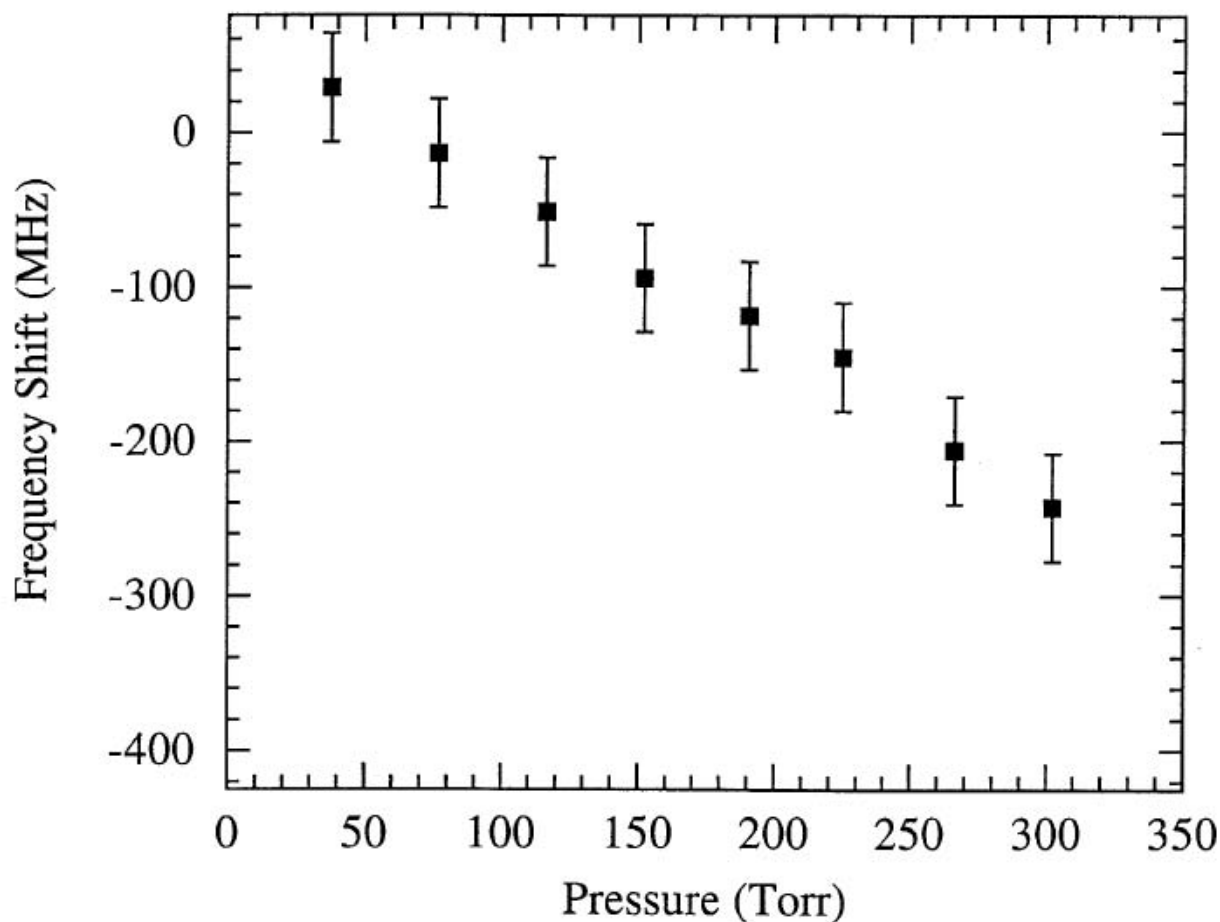


Fig. 5. 12692.67 cm⁻¹ acetylene absorption line-shift as varying the gas pressure at T = 294 K. The reference-cell gas pressure was 38 Torr and the pressure error was 5 Torr

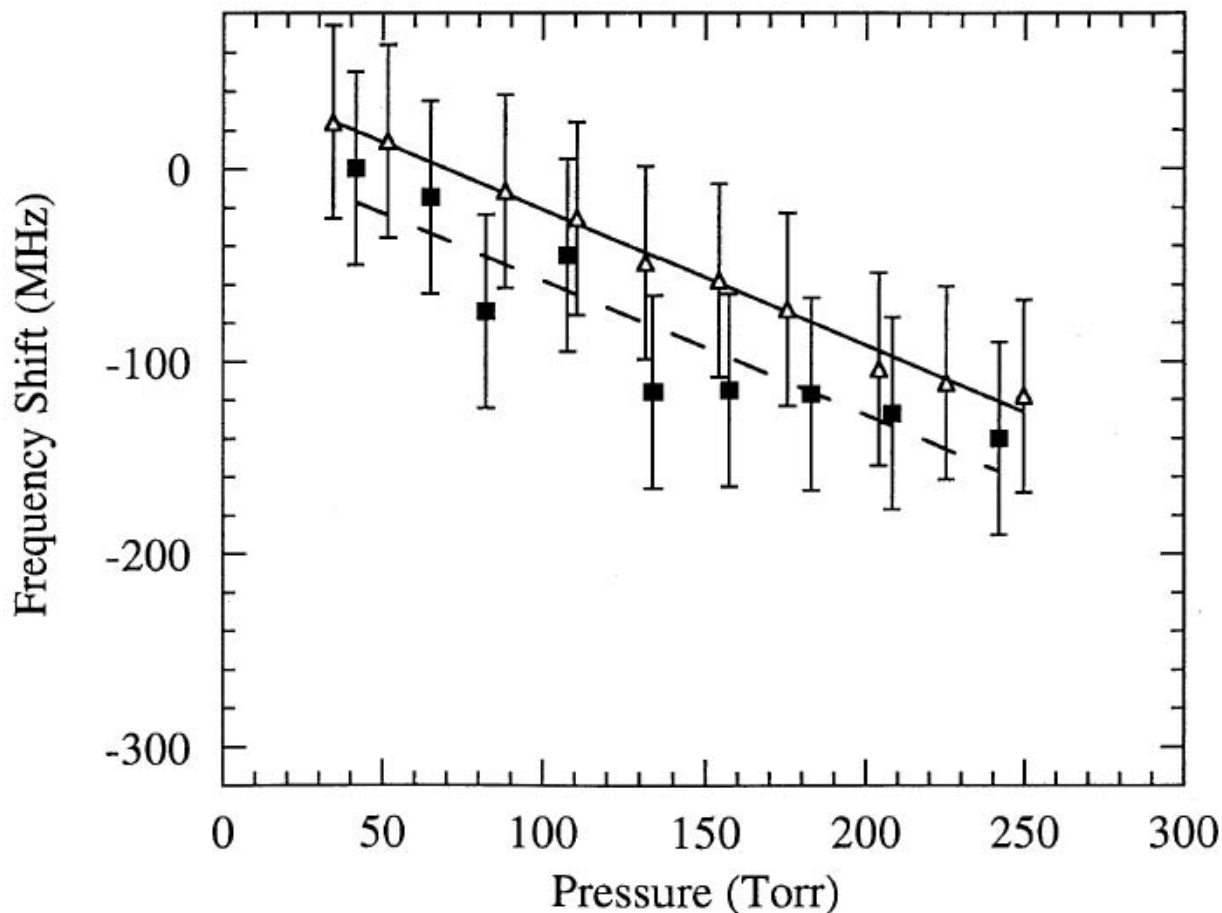


Fig. 6. Frequency shift of the 12714.73 cm^{-1} absorption line as varying the acetylene pressure. The error in pressure measurement was 5 Torr. The triangles refer to the DA measurements for which $S_{DA} = (-0.7 \pm 0.2)\text{ MHz/Torr}$. The filled squares are related to the WM measurements [$S_{WM} = (-0.7 \pm 0.3)\text{ MHz/Torr}$]. The best linear fits of the two sets of data are shown for comparison